Geoderma 432 (2023) 116398

Contents lists available at ScienceDirect

Geoderma

journal homepage: www.elsevier.com/locate/geoderma

Long-term tillage and irrigation effects on aggregation and soil organic carbon stabilization mechanisms

N. Dal Ferro [a,*], B. Stevenson [b], F. Morari [a], K. Müller [c]

[a] Department of Agronomy, Food, Natural Resources, Animals and Environment, Agripolis, University of Padova, Viale Dell'Università 16, 35020 Legnaro (Padova), Italy
[b] Land Use and Ecosystems Team, Manaaki Whenua Landcare Research, Hamilton, New Zealand
[c] Sustainable Production – Ruakura Research Centre, The New Zealand Institute for Plant & Food Research Ltd, Auckland, New Zealand

ARTICLE INFO

Handling Editor: Cornelia Rumpel

Keywords:
Complexed OC
Saturation threshold
Direct drill
Fines20
Fungal:Bacterial ratio

ABSTRACT

Sustainable soil management practices are required in agriculture to enhance carbon sequestration and restore soil functions. Here, the aim was to investigate the effect of different tillage practices combined with or without irrigation on (i) soil organic carbon (SOC) content, (ii) fungal biomass and their relationships with aggregate size classes in the soil surface layer; further, (iii) the concept of soil particle saturation with SOC was tested to evaluate if a threshold was reached in a 14 year-experiment. Our hypothesis was that long-term irrigation, intensive tillage and their combination, would negatively affect soil aggregation and SOC stabilization. The experiment has started in 2003 on a research farm in Canterbury, New Zealand. The present work focused on two contrasting tillage practices –intensive tillage with 20–25 cm ploughing (IT) and direct drill (DD)– combined with sprinkler-irrigated and non-irrigated (hereafter called Rainfed) conditions in a split-plot experimental design. Soil samples (0–5 cm layer) were analyzed for pore size distribution, specific surface area and microbial biomass. Further, wet sieving was used to isolate large macroaggregates (LM, > 2000 μm), small macroaggregates (SM, 250–2000 μm), microaggregates (m, 53–250 μm), particle sized silt + clay fractions (s+c, < 53 μm) and Fine20 particles (<20 μm), followed by the analysis of aggregate morphology and SOC quantification in them. Results showed that both DD and Rainfed management increased total SOC content of the bulk soil. Only the LM fraction and the SOC therein (OC-LM) increased significantly in DD compared to IT, while m and s+c fractions and OC-m and OC-s+c did not differ between treatments. Macroaggregate breakdown processes and measured SOC therein had likely not reached steady-state conditions, as suggested by the lack of any SOC differences in the aggregate size classes < 250 μm. In contrast, the Fines20:SOC ratio differentiated between soils that had reached (i.e., DD) or not reached (i.e., IT) the saturation threshold. Finally, it was observed that a higher fungal:bacteria (F:B) ratio was generally accompanied by a greater LM fraction and mean weight aggregate diameter, highlighting the importance of fungi in the formation of LM. These results suggested that our hypothesis of detrimental effects on soil aggregation and SOC accumulation of both tillage and irrigation was not fully demonstrated yet. A longer study period would be required to better understand the effects of such practices of SOC storage.

1. Introduction

Soil organic carbon (SOC) storage potential in agroecosystems has been largely investigated in the context of mitigating climate change and restoring soil functions (Chenu et al., 2018; Wiesmeier et al., 2019). To what extent agricultural soil management practices can increase SOC content is still debated, especially over longer time periods when SOC saturation may occur (Goh, 2004; Six et al., 2002; Stewart et al., 2007, 2008) as reported in several studies conducted, e.g., in Canada in a silty clay loam soil (Chung et al., 2008) and in a clay loam soil under permanent grassland in New Zealand (Kool et al., 2007). It follows that some agricultural practices may exhaust their potential for additional SOC accumulation and for this reason not be further supported.

Among soil properties, the presence of the fine mineral fraction is probably the most important to indicate a threshold beyond which additional SOC accumulation become ineffective (Wiesmeier et al.,

* Corresponding author.
E-mail address: nicola.dalferro@unipd.it (N. Dal Ferro).

https://doi.org/10.1016/j.geoderma.2023.116398
Received 26 July 2022; Received in revised form 17 February 2023; Accepted 18 February 2023
Available online 1 March 2023

2019). Dexter et al. (2008) identified a clay-to-carbon (clay:SOC) threshold of 10 in a wide range of arable and pasture soils of France and Poland, below which additional SOC would not be sequestered. At higher SOC content above a soil-specific saturation threshold, non-complexed organic carbon occurs and the effect of OC stabilization decreases (Dexter et al., 2008) without contributing further to carbon sequestration. In contrast, Hassink (1997) used fine particles < 20 μm (i.e., Fines20) and established a saturation threshold of 20 for Fines20:SOC by analysing a wide range of uncultivated and grassland topsoils of temperate and tropical regions. Hassink's approach was later tested in several cultivated soils and soil types (e.g. Cambisol), revealing that such relation was suitable to predict SOC sequestration potential (e.g., Wiesmeier et al., 2014; Zhao et al., 2006). Schjønning et al. (2012) investigated the interaction between fine mineral surfaces and SOC stabilization. The authors highlighted that the 2–20-μm fraction contributed significantly to soil specific surface area (SSA) and stabilized SOC stronger than clay alone. Moreover, complexed OC is a major driver controlling structure-related physical properties (e.g., porosity, bulk density) (Johannes et al., 2017).

In addition, physical SOC protection is exerted by macroaggregates (>250 μm) and microaggregates (<250 μm) therein (Six and Paustian, 2014). Soil aggregate, especially macroaggregate (Lehmann et al., 2017) formation has long been associated with fungal communities (both saprophytic and mycorrhizal) and their hyphae and exudates (e.g., glomalin associated with arbuscular mycorrhizal –AM– fungi) (Jastrow et al., 1998; Rillig and Mummey, 2006; Ritz and Young, 2004). The SOC residing within aggregates is physically protected due to decreased accessibility reducing SOC degradation phenomena (e.g., oxidation, microbial attack). The degree of soil aggregation –the level of soil particle arrangement and pore complexity– defines a maximum SOC storage capacity beyond which OC is not physically protected (Six and Paustian, 2014). These findings highlight that bulk soil has limits to the amount of SOC that can be protected. It depends not only on the intrinsic soil properties of different soil types, but it is also influenced by soil and land management strategies (Guo et al., 2020; Lugato et al., 2010; Stewart et al., 2007), which in turn can contribute to OC inputs and/or preservation/degradation of soil structure.

A number of soil management practices can enhance aggregate stabilization resulting in lower SOC turnover rates such as maintaining soil cover (Liu et al., 2005), the use of manure and plant residues (Almagro et al., 2017; Dal Ferro et al., 2012), the adoption of conservation tillage (Six et al., 2000) or the combination of different practices (e.g., Garcia-Franco et al., 2018). Especially by adopting no tillage, macroaggregates can be stabilized and in turn microaggregate-within-macroaggregate SOC protected. Conversely, microaggregate stability can only be marginally affected by the degree of tillage intensity, highlighting a different susceptibility to tillage-induced physical disturbance compared to macroaggregates (Balesdent et al., 2000).

Less is known about the effects of irrigation management on soil structure and SOC stabilization, despite irrigation has doubled in the last 60 years globally, and it is to date deployed on >20% of the cultivated land providing 40% of global food production (Rosa, 2022). The early results of Blanco-Canqui et al. (2010), where the effects of deficit irrigation on SOC content and on wet aggregate stability in croplands were studied in 5- to 8-year experiments, showed that the amount of macroaggregates increased with an increase of applied irrigation volumes (66 to 217 mm year^{-1}). The authors suggested that the stabilization of aggregates was due to an irrigation-induced increase in SOC content, which in turn was associated with the increase in biomass input and microbial-mediated organic binding agents. Hondebrink et al. (2017) investigated the effect of flood and drip irrigation on soil structure in organically and conventionally managed citrus orchards. The authors did not find significant differences in the stabilizing effect of aggregates when comparing irrigation treatments. Trost et al. (2013) found contrasting results in their literature review: in some studies irrigation was a driver of higher OC input, while in other studies greater SOC decomposition was observed due to enhanced microbial activity (Kochsiek et al., 2009; Zhou et al., 2016). An increased SOC loss was reported under New Zealand humid climate conditions, where a slight increase of C input due to irrigation was offset by a strong increase in SOC decomposition rates (Mudge et al., 2017; Whitehead et al., 2018). The combined effect of irrigation and tillage in croplands on SOC and soil architecture has not been sufficiently studied. Recent research by Pareja-Sánchez et al. (2017) highlighted a trade-off between topsoil structure degradation due to irrigation and structure preservation due to conservation tillage practices. However, these results should be tested with different crops and pedoclimatic conditions to evaluate their general validity. Improved soil structure conditions and enhanced SOC sequestration were found under drip irrigation when it was associated with plant residue incorporation and reduced tillage, compared with intensive tillage and flood irrigation in a 17-year-old citrus orchard experiment (Garcia-Franco et al., 2021). Potential effects of different land use practices on fungal biomass in relation to aggregate formation have been investigated. Garcia-Franco et al. (2015) studied the effect of afforestation in semiarid shrublands, reporting that a higher microbial biomass was related with enhanced SOC protection in microaggregates formed within macroaggregates. In contrast, in the study conducted by Daynes et al. (2013), it was found that arbuscular mycorrhizae were necessary to stabilize the newly formed structure into macroaggregates (>710 μm), but these were not necessary for structural development *per se*, which occurred when suitably nourished plants were present. But generally, this field of study has not yet been well investigated, especially the effects of site-specific conditions are still not well understood (Helgason et al., 2014). Recently, we studied the effect of 14 years of irrigation and tillage practices on topsoil structure using intact cores taken from a silty clay loam Cambisol in New Zealand (Müller et al., 2019). The experiment was set up to study the impact of growing farming practices that are being implemented in the agroecosystems. The irrigated agricultural land in New Zealand almost doubled between 2002 and 2019, from 384,000 to 735,000 ha, especially in the Canterbury region (Drewry et al., 2022), while conservation practices to minimize soil disturbance are included in national agricultural development programmes and increasingly adopted since 2008 (Kassam et al., 2019). Results obtained from macropore investigation (resolution = 30 μm) showed that intensive tillage (including 25-cm ploughing and disk cultivator) had negative effects on topsoil SOC content and soil functions (e.g., gas transport) compared with no tillage, while sprinkler irrigation had little effect on any of the parameters analyzed compared with rainfed conditions. However, the investigated pore network represented only a small portion (about 15%) of the total porosity. Therefore, we decided to broaden the analysis to the so far unexplored smaller soil aggregate compartments. We hypothesized that long-term irrigation and intensive tillage practices has negative effects on the intra-aggregate structure and affects the SOC accumulation and stabilization capacity. Using neutral lipid and phospholipid fatty acid (NLFA and PLFA) analyses, we also hypothesize that the relationships between saprophytic fungal biomass, fungal:bacterial ratio and AM fungal biomass under different tillage and irrigation treatments can affect soil aggregation. PLFA has been shown to be a good overall indictor of saprophytic and arbuscular mycorrhizal (AM) fungal biomass. For example, Bååth E and Anderson (2003) found a good correlation between the content of ergosterol (a fungal compound) and the PLFA 18:2w6,9. The neutral lipid fatty acid 16:1ω5*c* (Olsson, 1999; Olsson et al., 1995) has been found to be the preferred indictor for AMF fungi. Therefore, our aims were: (i) to investigate the single and combined effect of tillage and irrigation management on SOC-structure aggregate interaction; (ii) to identify whether a SOC saturation threshold occurred in a New Zealand arable soil after 14-year of continuous conservation tillage and/or irrigation practices, and (iii) to explore the role of fungi in soil aggregation.

2. Material and methods

2.1. Description of experimental site and soil sampling

The experimental site is located on a research farm of the Foundation for Arable Research in Chertsey, Canterbury, New Zealand (43°47′ S 171°58′ E, 109 m a.s.l.). The climate is temperate, with mean annual rainfall of 699 mm and mean annual temperature of 11.2 °C. Rainfall is evenly distributed throughout the year with a difference of about 20 mm between the driest and the wettest month. The soil is a silty clay loam Pallic Soil (Hewitt, 2010), which corresponds to a Cambisol (IUSS Working Group WRB, 2015). The main physical and chemical properties of the topsoil (0–10 cm) are reported in Table 1.

This long-term ongoing tillage and irrigation experiment was established in 2003 on a field with a history of mixed cropping and uniform tillage without irrigation. The crop rotation is typical for the Canterbury region involving wheat (*Triticum aestivum* L.), peas (*Pisum sativum* L.), ryegrass (*Lolium perenne* L.) and linseed (*Linum usitassimum* L.). At the time of sampling (see next paragraph), the soil was under the second year of ryegrass grown for seed. The experimental design is a split-plot experiment with two replications with irrigation management as main plot and different tillage intensities as split-plots, 25 m long × 12 m wide (Supplementary Fig. S1). The irrigation management factor includes two treatments within randomized blocks: a non-irrigated crop management –hereafter called "Rainfed"– and an irrigated crop management with a lateral travel spray irrigator –hereafter called "Irrigated". Over the years the irrigation was carried out according to the crop requirements that guaranteed a non-stress situation, with average water inputs of 130 mm year^{-1} distributed in four passes. The tillage management factor included six tillage intensities that were allocated randomly to each of the four main plots. In this study, the irrigation management factor was tested only in a factorial combination with the two most extreme tillage management practices to maintain continuity with previous experiments: the intensive tillage (IT) treatment, which included 20–25 cm depth ploughing followed by two passes of a Vaderstad Topdown cultivator (Väderstad Group, Sweden) and John Deere 750A (Deere & Company, USA) double disc drill; and the direct drill (DD) treatment, which was performed with a cross slot drill. No organic amendments were applied. Crop residues were left on the soil in DD and buried in the soil in IT. See the supplementary Fig. S1 for details about the experimental design and description of all the tillage treatments.

Soil samples were collected from four randomly selected locations in each split-plot in April 2017 and analyzed separately (2 irrigation × 2 tillage practices × 4 subsampling × 2 replicates). At each location, a disturbed bulk sample of about 1 kg and an undisturbed soil core (5 cm diameter × 5 cm length) were taken from the 0–5 cm layer to maintain continuity of analysis with previous studies (Müller et al., 2019) and emphasize the likely stratification effect due to different tillage practices. Soil cores were excavated by slowly pushing PVC cylinders into the soil. The soil samples were kept cool until delivery to the laboratory. Sub-samples of the bulk soil were freeze-dried and frozen at –80 °C before microbiological analysis. The remainder of the soil was air-dried and stored in a cool and dark place until analysis.

Table 1
Main soil physical and chemical properties of the topsoil (0–10 cm) at the experimental site in Chertsey, Canterbury, New Zealand. Mean values ± standard errors in brackets are reported.

Soil parameters	
Sand, 2000–50 μm (%)	10 (±1)
Silt, 50–2 μm (%)	50 (±1)
Clay, < 2 μm (%)	40 (±1)
pH	5.9 (±0.0)
Organic carbon (g kg^{-1})	26.8 (±0.7)
Total nitrogen (g kg^{-1})	2.3 (±0.1)
C/N	11.6 (±0.0)
Na^+ (mg kg^{-1})[a]	25.1 (±0.5)
K^+(mg kg^{-1})[a]	16.3 (±0.9)
Ca^{2+}(mg kg^{-1})[a]	280.6 (±13.5)
Mg^{2+}(mg kg^{-1})[a]	< 1.0 (±0.0)

[a]Exchangeable cations.

2.2. Soil particle size distribution, chemical and microbiological analyses

The soil texture was determined with laser diffraction (Malvern Mastersizer 2000; Malvern Instruments, Malvern, UK) of 2-mm sieved samples that were previously dispersed in a 2% sodium hexametaphosphate solution and shaken for 12 h at 80 rpm (Bittelli et al., 2019). Removal of SOC was carried out as a pretreatment before particle size analysis, by adapting the method proposed by Kunze and Dixon (1986). Soils were suspended in 250 ml of 15% H_2O_2 at room temperature and allowed to react until the end of gas development, followed by treatment with 30% H_2O_2 at 70 °C until the visible reaction ceased.

The non-fractionated soil was analyzed for organic carbon content (SOC, g kg^{-1}) by the flash combustion method using a CNS Elemental analyzer (Vario Max; Analysensysteme GmbH, Langenselbold, Germany), and the hot water extractable carbon (HWEC) was measured following Ghani et al. (2003). All wet sieved fractions (see paragraph 2.5 below) were also analyzed for organic carbon content and expressed as g OC kg^{-1} aggregate (Lugato et al., 2010; Simonetti et al., 2017).

A representative soil sample for each treatment was analyzed by X-ray powder diffraction (XRPD) to determine the mineral composition as in Piccoli et al (2016). Analyses focused on the identification of clay mineral phases in the bulk soil and in Fines20. X-ray diffraction data were collected using a Panalytical X'Pert PRO MPD diffractometer equipped with an X'Celerator detector, a Co-anode X-ray tube and operating in Bragg-Brentano reflection geometry. Quantitative estimates of individual minerals were obtained by full profile analyses of diffraction data applying the Rietveld method as implemented in Topas v4.1.

In addition, for assessing microbial community composition and biomasses of specific groups (e.g., total microbial, bacterial, fungal, Gram-positive, Gram-negative biomasses), we used phospholipid fatty acid (PLFA) analysis with quantification following the method of Bligh and Dyer (1959), as modified by White et al. (1979) and Bardgett et al. (1996). Briefly, lipids were extracted from 1.5 g of fresh soil, fractionated and methylated, and the resulting fatty acid methyl esters (FAMEs) analyzed using an Agilent 7890A GC with Agilent 5975C VL MSD (Agilent, Santa Clara, CA, USA). The neutral lipid and the phospholipid fractions were also analyzed. The resulting peaks were identified using retention times relative to two added internal standards (C13 and C19) and a bacterial methyl ester standard mixture (Supelco Bacterial Acid Methyl Esters CP Mix 47080-U; Sigma-Aldrich Corporation, St Louis, MO, USA). Peak size was quantified using the FAME 19:0 internal standard, and the abundance of each of the individual fatty acids extracted expressed as relative μg g^{-1} of dry soil using standard nomenclature and converted to μmol based on the molecular weight of the individual FAMEs. Microbial biomass was expressed as the sum of all FAME peaks.

Bacterial biomass was calculated from PLFAs associated with Gram-positive bacteria (i-15:0, a-15:0, i-16:0, i-17:0, and a-17:0), Gram-negative bacteria (cy-17:0, cy-19:0, 16:1 ω7c and 18:1ω7c) (Waldrop and Firestone, 2004; Zelles, 1999), and the general bacterial marker 15:0 (Bardgett et al., 1996). Relative biomass (i.e., percentage of community composition) for each biomarker was determined by dividing the absolute biomass by the total PFLA biomass. The fungal PLFA marker (18:2ω6,9c) was used to calculate saprophytic fungal biomass and the fungal:bacterial (F:B) ratio. The arbuscular mycorrhizal fungal biomass was calculated from the 16:1ω5c NLFA marker.

2.3. Mercury intrusion porosimetry

Accessible porosity and pore size distribution within the diameter

range of 0.0074–100 μm were measured with a Thermo Finnigan (Waltham USA) Pascal 140 (3.8–100 μm) and Pascal 240 (0.0074–15 μm). The pore radius (R) was calculated using the Young-Laplace equation:

$$R = \frac{2\gamma\cos\theta}{P} \quad (1)$$

where γ is the mercury surface tension (0.47 N m^{-1}), P is the pressure with which mercury intrudes and θ is the contact angle between soil and mercury (140°). Pores were classified as macropores (100–75 μm, m^3 m^{-3}), mesopores (75–30 μm, m^3 m^{-3}), micropores (30–5 μm, m^3 m^{-3}), ultramicropores (5–0.1 μm, m^3 m^{-3}) and cryptopores (0.1–0.0074 μm, m^3 m^{-3}) (Cameron and Buchan, 2006).

2.4. Gas adsorption

The Brunauer-Emmett-Teller (BET) specific surface area (SSA) of bulk samples (about 3 g) was determined using the linear part of the N_2 isotherm (between pressure p/p_0 0.05 and 0.35) obtained with a Sorptomatic 1990 at a temperature of −195.15 °C, after degassing the sample at 105 °C overnight. To quantify the SOC coating effect on fine soil particles and possible SOC saturation mechanisms, a selection of four out of 32 samples from different treatments was subjected to further SSA analysis after SOC removal (Kunze and Dixon, 1986), being organic matter covering soil particles, thereby reducing the effective measured surface area (Schjønning et al., 2012).

2.5. Wet aggregate fractionation

The soil aggregate size classes were separated using a wet-sieving method adapted from Elliott (1986). After manually breaking the undisturbed samples, about 50-g of soil was homogeneously selected with a Sample Divider PT 100 (Retsch GmbH, Haan, Germany), from which 8-mm sieved soil was immersed in distilled water for 5 min on top of a 2000-μm sieve for slaking. Water-stable large macroaggregates (LM, 2000–8000 μm) were first isolated by oscillating manually the sieve 3 cm up and down for 50 times in about 2 min. Correction for elementary particles > 2000 μm was not necessary because they contained none. The free floating particulate organic matter was removed before further fractionation and not included in the analysis (Cambardella and Elliott, 1992). The water-stable LM aggregates were then separated into three aggregate-size fractions by wet-sieving using an automatic machine oscillator (Simonetti et al., 2017). The apparatus produces 3-cm stroke vertical movements to overlapping sieves with 250- and 53-μm mesh. The sieves, 10 cm in diameter and 5 cm height, were immersed in distilled water inside a beaker (15 cm diameter × 18 cm height). Prior to sieving, the water level was adjusted to prevent water flowing over the edge of the 250-μm sieve during the oscillation. Aggregates were separated by vertical oscillations at a frequency of 50 rpm for 18 min (900 oscillations in total). Small macroaggregates (SM, 2000–250 μm) and microaggregates (m, 250–53 μm) were collected from the sieves, while the silt–clay fraction (s+c, <53 μm) remaining in the beaker was precipitated by adding 3 ml of 1 N $CaCl_2$. All isolated fractions were dried at 50 °C in a forced-air oven and weighed. As a measure of soil structural stability, the mean weight diameter (MWD, μm) was calculated according to Kemper and Rosenau (1986).

Additionally, a soil fraction of primary particles < 20 μm (hereafter, Fines20) was isolated from 15-g homogeneous bulk samples. First, the soil material was dispersed in a 1-litre solution of sodium hexametaphosphate for 24 h, thereafter it was washed with distilled water on a 20-μm mesh sieve, and the material passing the sieve was collected, oven-dried at 50 °C, weighed and stored for further analysis.

2.6. Aggregate morphology

An automated particle characterization-optical microscope system (Morphologi G3, Malvern Instruments Ltd, Malvern, UK) was used to determine the mean diameter and morphologic properties of SM (2000–250 μm), m (250–53 μm) and s+c (<53 μm) aggregate size classes. The instrument produced a detailed analysis by automatically capturing images of the sample scanned with microscopic optics. Prior to analysis, a minimum of 150 aggregates for each sample was distributed manually on to a glass plate to maximize physical separation between fractions and to avoid their contact. Only aggregates that kept separate from each other were analyzed. The optics of the instrument were set as follows: 2.5× (SM), 10× (m), 50× (s+c) magnification objectives with an episcopic light mode and an exposure of 100 ms, enhanced with automated "particle stitching" to recognize aggregates occupying two or more frames that could be "stitched" together to extract the entire "edge-stitched" aggregate. The focus and threshold were set manually before each measurement by minimizing the blurring effects on aggregate edges and maximizing the contrast between the aggregates and the background. Aggregate mean diameter was calculated as the equivalent circle diameter (*ECD,* μm) (i.e., the diameter of a circle with the same area (A) of the 2-D image of the object) according to the equation below:

$$ECD = 2\sqrt{\frac{A}{\pi}} \quad (2)$$

Circularity (*Circ*), a measure of how well an object approximates a perfect circle, was calculated as follows:

$$Circ = \frac{2\pi A}{P^2} \quad (3)$$

where A (μm^2) is the particle area and P (μm) is the particle perimeter. Circularity ranged between 0 and 1, where 1 corresponds to a perfect circle while irregular objects approached 0.

Convexity (*Cx*) measures the edge roughness of a particle, and is the ratio between the convex hull perimeter *(Pc*) and the actual perimeter of an object:

$$C_x = \frac{P_c}{P} \quad (4)$$

Convexity ranged between 0 and 1. An object with a convexity of 1 indicates a smooth shape because the convex hull perimeter equals the actual perimeter.

Solidity (*S*), a measure of the overall concavity of a particle, is obtained as the ratio between the area of the object and the area enclosed by the convex hull (*Ac*):

$$S = \frac{A}{A_c} \quad (5)$$

Solidity values range between 0 and 1. A more solid object produces a more similar image and convex hull areas, and results in a solidity value that approaches 1. Elongation index (*Ei*), a measure of the overall symmetry or asymmetry of an object, is determined by:

$$E_i = 1 - \frac{width}{length} \quad (6)$$

where width (μm) and length (μm) are the shortest and longest object axes, respectively. Elongation indicates the symmetry (close to 0) or asymmetry (close to 1) of an object in all directions. Details about shape parameters are reported in Supplementary Table S1.

2.7. SOC saturation threshold estimation

According to previous studies (Schjønning et al., 2012), a distinction between soils with fully complexed OC (Fines20:SOC > 20) and soils with additional OC beyond the maximum theoretical complexation level

(Fines20:SOC < 20) –i.e. beyond a saturation threshold– can be estimated. The non-complexed OC (nOC) concentration can therefore be differentiated from the fully complexed OC (cOC). If measured OC > theoretical OC (calculated as Fines20/20), then:

$$nOC = SOC - Fines20/20, \quad (7)$$

$$\text{and } cOC = SOC - nOC. \quad (8)$$

If OC < theoretical OC, then:

$$nOC = 0, \quad (9)$$

$$\text{and } cOC = \text{measured OC}. \quad (10)$$

2.8. Statistical analysis

To account for the split-plot design with subsampling of the experiment, data were analyzed with ANOVA derived from linear mixed-effect model. The linear model represented the hierarchical structure of four subsamples, γ_l, nested in subplots, β_k, (IT, DD), nested in main plots, α_i, (Rainfed, Irrigated), and main plots finally nested in blocks, τ_l. Fixed effects were tillage and irrigation managements, while random effects were subsamples, replicates, and their interaction with experimental variables, following the expression: $y_{ijkl} = \mu + \alpha_i + \beta_j + \gamma_k + \tau_l + (\alpha\beta)_{ij} + \delta_{il} + \zeta_{ijl} + \varepsilon_{ijkl}$; where y_{ijkl} is the measured response, and δ_{il}, ζ_{ijl}, and ε_{ijkl} denote experimental error terms associated with the main plot factor, the subplot factor, and the subsampling, respectively. Variability associated with the modelled means was provided by the Tukey's HSD (honestly significant difference) test at the 5% level of significance. The homogeneity of variance was assessed with the Bartlett's test. An additional mixed model was applied to disentangle the influence of combined management practices and F:B ratio on aggregate size class formation, SOC and MWD. The model considered the F:B ratio as continuous factor, while the factorial combination of tillage and irrigation were included as categorical factor. Moreover, the relationship between complexed and non-complexed OC and pore size classes were analyzed with linear regressions models and considered significant at $p < 0.05$. Data analysis was done using JMP Pro version 17.0.0 (JMP Statistical Discovery LCC).

3. Results

3.1. Soil particle characterization

The sand (50–2000 μm), silt (50–2 μm), and clay (<2 μm) particle size distributions were on average 10 ± 1%, 50 ± 1% and 40 ± 1%, respectively and similar for all treatments (Table 2). Significant differences in specific surface area were observed between tillage treatments, with higher values in IT (5.33 ± 0.30 $m^2\ g^{-1}$) than DD (3.89 ± 0.22 $m^2\ g^{-1}$). The removal of organic matter from soil particles resulted in a 35% increase in the detected SSA (on average 7.18 *vs.* 4.61 $m^2\ g^{-1}$), highlighting the higher OC coverage in the DD soils that had significantly higher SOC content than IT. Values of SSA after SOC removal varied between 6.88 and 8.40 $m^2\ g^{-1}$. Fine particles < 20 μm (Fines20) ranged between a minimum of 44.4% and a maximum of 57.4%. On average, Fines20 were 52.7% of the total soil particles. Notably, some significant differences were observed between treatments, with a lower percentage of Fines20 under DD (51.4 ± 0.8%) than under IT (53.9 ± 0.7%).

X-ray powder diffraction analysis showed similar clay mineralogical composition of all soil samples (Table 3). The soil was dominated by 2:1 layer clay mineral, mainly muscovite/illite (weight fraction > 15%), followed by 2:1:1 layer chlorite (weight fraction > 5%). Residual primary minerals –quartz and feldspar– were also detected in the clay fraction, while other clay minerals such as 1:1 layer kaolinite, or smectite and vermiculite were not detected. The detection of Natron

Table 2
Particle size distribution, specific surface area (SSA), soil organic carbon (SOC) and hot water extractable carbon (HWEC) contents of bulk soil samples under different irrigation and tillage intensity treatments. The percentage of fine particles < 20 μm (Fines20) and the OC-Fines20 (g kg^{-1}) are also reported. Values in each column followed by different letters were significantly different ($p < 0.05$). Mean values ± standard errors in brackets are reported.

		Sand (%)		Silt (%)		Clay (%)		SSA ($m^2\ g^{-1}$)		Fines20 (%)		SOC (g kg^{-1})		HWEC (μg C g^{-1})		OC-Fines20 (g kg^{-1})	
Irrigated	DD[a]	11	(±2)	49	(±1)	40	(±1)	4.14	(±0.25)	53.0	(±0.8)	29.4	(±0. 25)	1076	(±20)	28.7	(±0.14)
	IT	9	(±1)	50	(±1)	41	(±1)	5.39	(±0.53)	53.6	(±1.1)	22.4	(±0. 61)	634	(±32)	23.7	(±0.11)
Rainfed	DD	12	(±1)	50	(±1)	38	(±1)	3.65	(±0.35)	49.8	(±1.3)	30.9	(±0. 54)	1099	(±17)	30.2	(±0.19)
	IT	10	(±1)	49	(±1)	41	(±1)	5.26	(±0.32)	54.1	(±0.7)	24.3	(±0. 45)	733	(±27)	26.0	(±0.09)
-																	
DD		12	(±1)	50	(±1)	39	(±1)	3.89	b (±0.22)	51.4	b (±0.8)	30.1	a (±0.35)	1088	a (±24)	29.4	a (±1.17)
IT		10	(±1)	49	(±0)	41	(±1)	5.33	a (±0.30)	53.9	a (±0.7)	23.4	b (±0.95)	683	b (±13)	24.9	b (±0.77)
-																	
Irrigated		10	(±1)	49	(±1)	40	(±1)	4.77	(±0.33)	53.3	(±0.7)	25.9	b (±0. 95)	855	b (±60)	26.2	(±1.10)
Rainfed		11	(±1)	50	(±1)	39	(±1)	4.45	(±0.31)	52.0	(±0.9)	27.6	a (±0. 91)	916	a (±49)	28.1	(±1.17)

[a]DD, direct drill; IT, intensive tillage.

Table 3
Estimation of relative weight fractions (wt%) of mineral phases in bulk samples and in Fines20. Mean values ± standard errors in brackets are reported.

Phase	DD wt%		IT wt%		DD-Fines20 wt%		IT-Fines20 wt%	
Quartz	42.4	(±0.2)	41.7	(±0.1)	33	(±0.2)	38.9	(±0.2)
Feldspar	37.4	(±0.4)	37.2	(±0.4)	38.6	(±0.4)	36.2	(±0.4)
Chlorite	5.1	(±0.1)	6.2	(±0.1)	6.1	(±0.2)	5.5	(±0.2)
Muscovite/Illlite	15.0	(±0.2)	15.0	(±0.2)	18.7	(±0.2)	16.4	(±0.2)
Natron, $Na_2(CO_3)•10(H_2O)$	–		–		3.4	(±0.2)	3.1	(±0.2)

($Na_2(CO_3)•10(H_2O)$) in the Fines20 fraction is an artefact due to the dispersing solution used.

3.2. Bulk soil organic carbon content and microbial community

Soil organic carbon (SOC) content in the bulk topsoil was affected by tillage and by irrigation management. Significant higher values were observed under DD than IT, with average values of 30.1 ± 0.3 and 23.4 ± 0.4 g kg^{-1}, respectively. The Rainfed treatment had SOC = 27.6 ± 0.9 g kg^{-1} while the Irrigated treatment's SOC was 25.9 ± 0.9 g kg^{-1} ($p < 0.05$). Similar results were found for the hot water-extractable carbon (HWEC) (Table 2), which was strongly correlated with SOC (r = 0.97). With regard to OC-Fines20, it was found that IT had significantly lower SOC than DD, 24.9 ± 0.77 *vs*. 29.4 ± 1.17 g kg^{-1}, respectively (Table 2).

For total PLFA biomass (as a measure of microbial biomass) there was a significant effect of tillage intensity with DD having greater average PLFA biomass (146 ± 3 nmol g^{-1} soil) than IT (96 ± 4 nmol g^{-1} soil), but irrigation treatment did not have a significant effect (Table 4). Both absolute bacterial and fungal biomass were greater under DD (Table 4), but the proportional representation of each in the community did not follow the same pattern (Table 4). The relative bacterial biomass (i.e., percent of the total PLFA biomass) was greater under IT than DD and greater under Irrigated than Rainfed. Both the relative fungal biomass and fungal:bacterial (F:B) ratio were significantly greater with average values of 2.76% ±0.15 and 0.057% ±0.003 of total PLFA biomass under DD than IT treatments (2.01% ±0.12 and 0.040% ±0.002), respectively, but there was no overall irrigation effect. The AM fungal biomass, however, was greater under Irrigated than under Rainfed (average values, 6.82 ± 1.06 and 3.06 ± 0.43) with no significant tillage effect.

3.3. Aggregate total porosity and pore size distribution

Total porosity was not significantly affected by the treatments. It ranged between a minimum of 0.36 m^3 m^{-3} for Irrigated IT and a maximum of 0.45 m^3 m^{-3} for Rainfed DD and averaged 0.40 m^3 m^{-3}. Ultramicropores (5–0.1 μm) dominated and accounted for 66.3% of the total porosity, followed by micropores (30–5 μm; 18.3%). The remaining 15.5% was formed by macropores (100–75 μm, 6.2%), mesoporoses (75–30 μm, 5.5%) and cryptopores (0.01–0.0074 μm, 3.7%). The only significant difference in porosity between treatments was observed for micropores (30–5 μm), where it was lower under DD (0.02 m^3 m^{-3}) than IT (0.03 m^3 m^{-3}), and for ultramicropores (5–0.01 μm). Direct drill (Irrigated and Rainfed) and IT (Rainfed) treatments had a significantly larger ultramicroporosity (0.27 m^3 m^{-3}, on average) than Irrigated IT

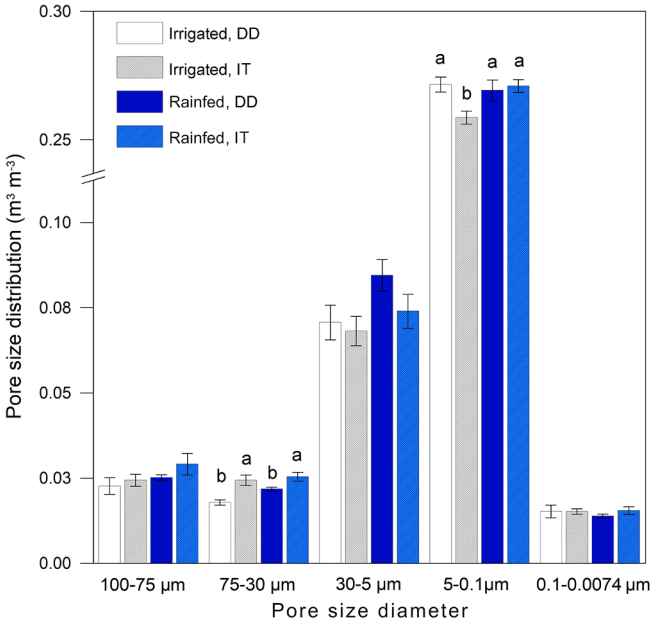

Fig. 1. Pore size distribution (m^3 m^{-3}) in the diameter range 100–0.0074 μm under different management practices: Irrigated and Rainfed, intensive tillage (IT) and direct drill (DD). Columns labelled with different letters within the same pore size class indicate significant differences ($p < 0.05$).

Table 4
Total, bacterial (B) and fungal (F) biomass amounts assessed via neutral lipid and phospholipid fatty acid (NLFA and PLFA) analyses under different irrigation and cultivation intensity systems. Values in each column followed by different letters were significantly different ($p < 0.05$). Mean values ± standard errors in brackets are reported.

	Total PLFA	Bacterial biomass	Fungal biomass	Bacterial biomass	Fungal biomass	F:B ratio	AM Fungi[b]
	(nmol g^{-1} soil)	(nmol g^{-1} soil)	(nmol g^{-1} soil)	(% of total PLFA)	(% of total PLFA)		(nmol g^{-1} soil)
Irrigated-DD[a]	147 (±5)	73 (±2)	4 (±0)	49.4 (±0.4)	2.60 (±0.19)	0.053 (±0.004)	5.16 (±0.87)
Irrigated-IT	97 (±7)	50 (±3)	2 (±0)	51.9 (±0.2)	1.99 (±0.16)	0.038 (±0.003)	8.48 (±1.81)
Rainfed-DD	146 (±4)	69 (±2)	4 (±0)	47.4 (±0.5)	2.92 (±0.24)	0.062 (±0.005)	3.38 (±0.74)
Rainfed-IT	102 (±5)	50 (±2)	2 (±0)	49.4 (±0.5)	2.03 (±0.18)	0.041(±0.004)	2.74 (±0.50)
-							
DD	146 (±3) a	71 (±2) a	4 (±0) a	48.4 (±0.4) b	2.76 (±0.15) a	0.057 (±0.003)	4.27 (±0.60) b
IT	99 (±4) b	50 (±2) b	2 (±0) b	50.6 (±0.4) a	2.01 (±0.12) b	0.040 (±0.002)	5.61 (±1.17) a
-							
Irrigated	122 (±8)	61 (±3)	3 (±0)	50.6 (±0.4) a	2.30 (±0.14)	0.046 (±0.003)	6.82 (±1.06)[c]
Rainfed	124 (±7)	60 (±3)	3 (±0)	48.4 (±0.4) b	2.47 (±0.19)	0.051 (±0.004)	3.06 (±0.43)

[a]DD, direct drill; IT, intensive tillage.
[b]As represented by the neutral lipid 16:1ω5c marker.
[c]Irrigation was considered marginally significant ($p = 0.056$) for the AM fungal marker.

treatments (0.26 m^3 m^{-3}) (Fig. 1).

3.4. Soil aggregate size classes

The large macroaggregate size class (LM, 2000–8000 μm) was significantly affected by tillage intensity, with increasing values under DD (57%) than IT (29%) treatments ($p < 0.05$). Results were opposite in smaller aggregate size classes, with IT that tended to be greater than DD in SM (41% *vs.* 28%), m (20% *vs*. 9%), and s+c (10% *vs*. 6%) (Table 5). Regarding the irrigation treatment, LM tended to be greater under Irrigated (50%) compared to Rainfed (36%) management as opposed to SM, m, and s+c that slightly increased in Rainfed than Irrigated conditions.

For tillage intensity, SOC content also differed between aggregate size classes (Table 6) with significant higher values ($p < 0.05$) that were observed in OC-LM (30.0 g kg^{-1}) under DD than IT (24.1 g kg^{-1}, on average). Similar SOC content was found between irrigation managements, with differences between size classes of 0.3 (OC-LM), 0.2 (OC-SM), 0.1 (OC-m) and 1.0 (OC-s+c) g kg^{-1} between Irrigated and Rainfed treatments (Table 6).

3.5. Aggregate morphology

Aggregate shape, captured through optical microscope images (Fig. 2), reveals differences between tillage treatments. Aggregates tended to be rounder and smoother under IT than DD due to the mechanical soil disturbance. A visual inspection showed differences in both SM and m shape, with more circular aggregates without protrusions under IT than DD. In fact, the quantitative analysis on 2D images showed higher circularity and solidity (*S*) for IT compared with DD. The IT treatment generated more rounded shapes with a marked convex closure as well as a higher convexity (*Cx*), meaning that aggregates were free of irregular features that would be reflected in a higher roughness (Table 7). By contrast, the m tended to be rougher (high *Cx*) under IT than under DD. Significant differences were not detected in the s+c.

Table 5
Mean weight proportion of soil aggregate size classes under different irrigation and tillage intensity treatments. Values in each column followed by different letters were significantly different ($p < 0.05$). Mean values ± standard errors in brackets are reported.

	Mean weight proportion (%)			
	LM[b]	SM[c]	m[d]	s+c[e]
Irrigated-DD[a]	66 (±4)	24 (±2)	6 (±1)	4 (±0)
Irrigated-IT	35 (±4)	40 (±2)	19 (±3)	6 (±2)
Rainfed-DD	48 (±6)	33 (±4)	12 (±2)	7 (±2)
Rainfed-IT	24 (±4)	42 (±4)	21 (±3)	13 (±3)
-				
DD	57 (±4) a	28 (±2)	9 (±1)	6 (±1)
IT	29 (±3) b	41 (±2)	20 (±2)	10 (±2)
-				
Irrigated	50 (±5)	32 (±3)	13 (±2)	5 (±1)
Rainfed	36 (±5)	37 (±3)	17 (±2)	10 (±2)

[a]DD, direct drill; IT, intensive tillage.
[b]LM, Large macroaggregates (2000–8000 μm).
[c]SM, Small, macroaggregates (2000–250 μm).
[d]m, microaggregates (250–53 μm).
[e]s+c, Silt-clay fraction (<53 μm).

3.6. Relationship between soil particles, SOC concentration and fungal communities

Our main interest in measuring the fungal biomass and fungal:bacterial (F:B) ratios was to determine whether there were relationships between the fungal components and aggregate size classes (and subsequently the carbon concentrations within those size classes). Significant ($p < 0.05$) but weak linear regressions up to a maximum $R^2 = 0.36$ were found between microbiological parameters (fungal:bacterial ratio, relative fungal biomass) and LM, OC-LM and MWD. When the interaction between tillage and irrigation management were considered, linear regression models showed that the F:B ratio increased the explained variance up to 58% in the LM and 56% of the variance in MWD (Fig. 3A and 3C; Supplementary Table S2-S3) under Rainfed-IT. The F:B ratio also explained 48% of the variance in OC-LM (Fig. 3B; Supplementary Table S2-S3) under the same treatment combination. As can be seen in Fig. 3A, the interaction between Irrigated management and DD treatment showed a distinctly different trend compared to other treatments for the relationship between F:B and LM, which decreased with increasing F:B ratio. However it is important to note that both OC-LM and MWD still appear to be increasing with F:B within these treatments (Fig. 3B and 3C).

3.7. Relationship between soil particles and SOC concentration

The relationship between SOC content and fine particles was used to describe the maximum amount of SOC that can be permanently complexed in soils. The ratios clay:SOC (Dexter index) and Fines20:SOC (Hassink index) were 15.2 ± 0.5 and 20.1 ± 0.6, on average, with values below the respective SOC saturation thresholds, which denotes the saturation of exchange sites, of 10 (Dexter index) and 20 (Hassink index) in just one and 16 of 32 cases for the clay:SOC and Fines20:SOC ratios, respectively (Fig. 4A,B). To note is that such differentiation was mainly due to different tillage treatments: in particular all samples with ratios

Table 6
Organic carbon concentration within the different soil aggregate size classes under different irrigation and tillage intensity treatments. Values in each column followed by different letters were significantly different ($p < 0.05$). Mean values ± standard errors in brackets are reported.

	OC concentration (g C kg^{-1} aggregate)			
	OC-LM[b]	OC-SM[c]	OC-m[d]	OC-s+c[e]
Irrigated-DD[a]	30.3 (±1.2)	26.5 (±1.4)	22.7 (±0.9)	17.9 (±0.9)
Irrigated-IT	23.6 (±1.7)	24.7 (±2.2)	21.8 (±1.8)	17.8 (±1.2)
Rainfed-DD	29.8 (±1.0)	25.9 (±0.8)	21.9 (±0.7)	17.7 (±0.4)
Rainfed-IT	24.7 (±0.5)	25.7 (±1.0)	22.8 (±0.8)	19.8 (±1.2)
-				
DD	30.0 (±0.8) a	26.2 (±0.8)	22.3 (±0.6)	17.8 (±0.5)
IT	24.1 (±0.9) b	25.2 (±1.2)	22.3 (±1.0)	18.8 (±0.9)
-				
Irrigated	26.9 (±1.3)	25.6 (±1.3)	22.2 (±1.0)	17.8 (±0.7)
Rainfed	27.2 (±1.3)	25.8 (±0.6)	22.3 (±0.5)	18.8 (±0.7)

[a]DD, direct drill; IT, intensive tillage.
[b]OC-LM, organic carbon content (g kg^{-1}) associated with large macroaggregates (2000–8000 μm).
[c]OC-SM, organic carbon content (g kg^{-1}) associated with small, macroaggregates (2000–250 μm).
[d]OC-m, organic carbon content (g kg^{-1}) associated with microaggregates (250–53 μm).
[e]OC-s+c, organic carbon content (g kg^{-1}) associated with silt–clay fraction (<53 μm).

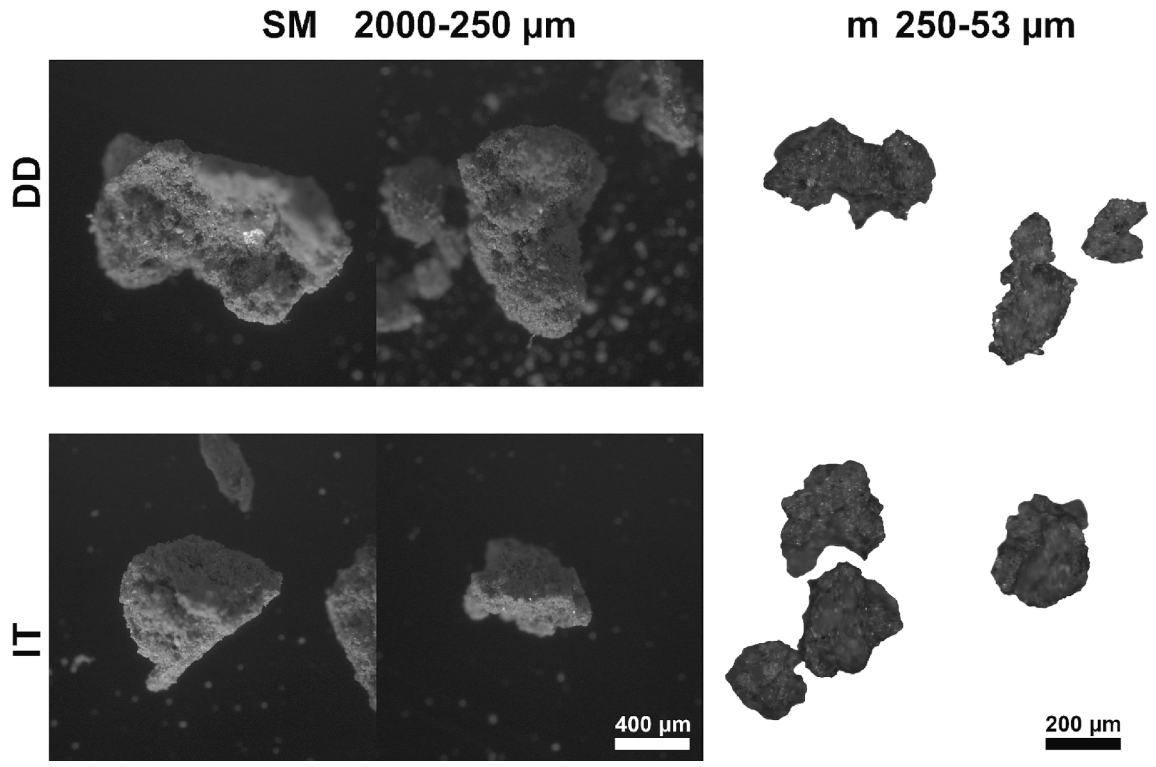

Fig. 2. Visualization of small macroaggregates (SM, 2000–250 µm) and microaggregates (m, 250–53 µm) with Morphologi G3 optical microscope selected from intensive tillage (IT) and direct drill (DD) management practices.

Table 7
Average morphology parameters and images of selected representative aggregates under different tillage practices (DD, direct drill; IT, intensive tillage) in the different aggregate size fractions, SM (small, macroaggregates, 2000–250 µm), m (microaggregates, 250–53 µm) and s+c (silt–clay fraction, < 53 µm). Values labelled with asterisks were significantly different ($p < 0.05$).

	Morphology parameters[a]	DD[b]	IT[b]		DD	IT
SM	ECD (µm)	476	410			
	Circularity	0.756	0.767	*		
	E_i	0.234	0.220			
	S	0.949	0.953	*		
	C_x	0.936	0.937	*		
m	ECD (µm)	136	128			
	Circularity	0.696	0.703			
	E_i	0.255	0.247			
	S	0.924	0.928			
	C_x	0.917	0.918	*		
s+c	ECD (µm)	16	15			
	Circularity	0.721	0.710			
	E_i	0.263	0.266			
	S	0.957	0.951			
	C_x	0.912	0.910			

[a]ECD, equivalent circle diameter; E_i, elongation index; S, solidity, C_x, Convexity.

below the Hassink index threshold were from the DD treatment (Fig. 4B). The dashed lines in Fig. 4A and B indicate the division of clay (Fig. 4A) or Fines20 (Fig. 4B) and total SOC as suggested by Dexter et al. (2008) and Hassink (1997), respectively. Notably, in Fig. 4A the separations between DD and IT were identical when increasing the Dexter index threshold to 14 (dotted line).

Significant positive relationships were observed between the bulk SOC content and LM, as well as between SOC and the OC-Fines20 (Fig. 4

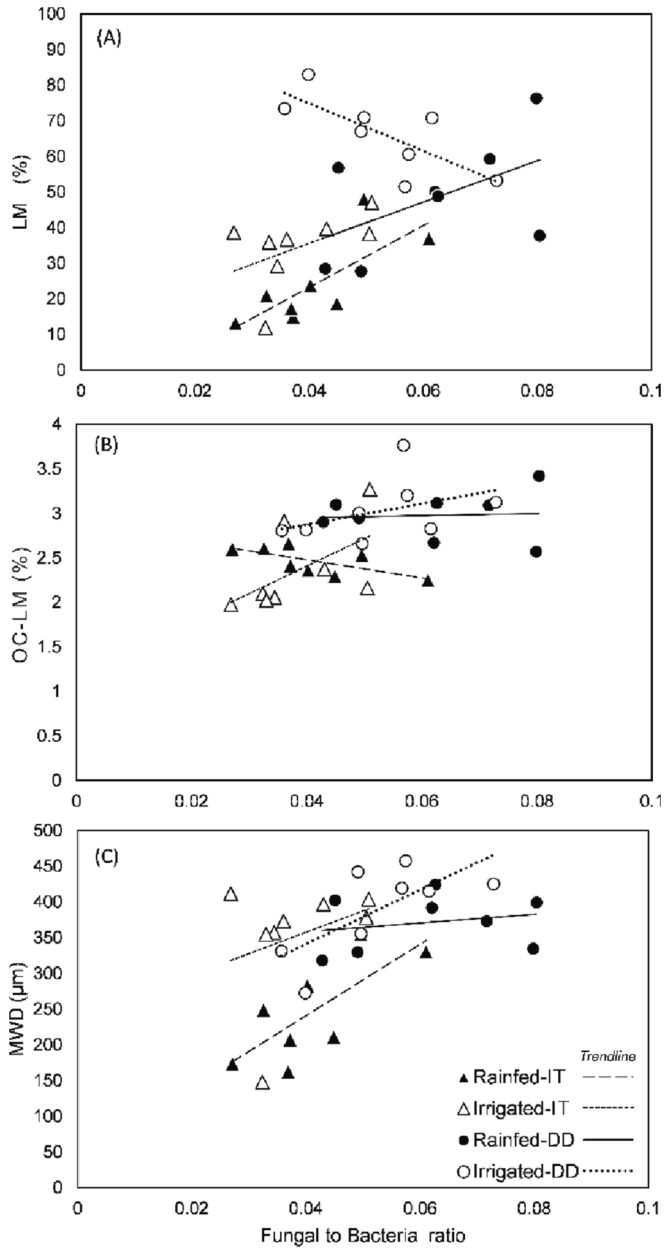

Fig. 3. Relationship between fungal to bacteria ratio (derived from PLFA analysis) and (A) percentage of aggregates > 2000 μm (LM), (B) percentage of soil organic carbon (SOC) in aggregates > 2000 μm (OC-LM), and (C) mean weight diameter (MWD) derived from aggregate size distribution under different management practices: Irrigated and Rainfed, intensive tillage (IT) and direct drill (DD). Data points represent individual sampling points. Linear regression equations and significance are reported in Supplementary Table S2.

C,D). In the latter the scatter around the regression line deteriorates the predictive power of the model, however a saturation threshold between Fines20 and OC-Fines20 was observed, as described by the nonlinear polynomial model ($y = -0.85x^2 + 5.17x - 4.90$; $p < 0.01$).

Regression analyses between complexed (Fig. 5A) and non-complexed OC concentrations (Fig. 5B), and pore size classes allowed to identify differences in soil structure of OC-unsaturated and OC-saturated soils, respectively: in the first case, the SOC concentration above the Hassink index threshold (complexed OC) predicts soil structural changes (Fig. 5A), while the same effects on soil structure were not observed when the soil had SOC beyond the saturation threshold (i.e. non-complexed OC; Fig. 5B). In particular, the larger the potentially complexed OC concentrations –which means that more free fine particles occurred– the more pores were in the range 30–75 μm and fewer pores were in the range 30–0.1 μm. Conversely, when the fine particles were all C-saturated –which means that free fine particles did not occur– and non-complexed OC is expected, a pore-mediated soil structural change was not observed, suggesting that a change of soil structure occurs primarily when an interaction between fine particles and OC takes place. No differences in pore structure were found when non-complexed OC content was estimated from the Dexter index threshold (data not shown).

4. Discussion

4.1. Long-term tillage effects on soil aggregation, SOC content and microbial community

After 14 years of combining different tillage and irrigation treatments of a Cambisol under cropping, some differences were observed in the aggregate classes and their OC content. The tillage intensity had the largest effect and resulted in more LM (>2000 μm) under DD than IT, and simultaneously increased the SOC content of LM. In contrast, the slight increase in SM under IT than under DD was not reflected in differences in OC. No further differences in the smaller aggregate size classes were observed between different tillage treatments. The positive effect of reduced tillage intensity on soil aggregation was frequently reported in previous papers (Chung et al., 2008; Sithole et al., 2019), suggesting potential limits for soil aggregation under intensive tillage, and thus, for the physical protection of SOC.

Interestingly, the link between soil aggregate size and fungal biomass and/or PLFA indicators (i.e. fungal to bacterial ratio) that were observed in this study has been also been made in other recent papers (Jiang et al., 2011; Liao et al., 2020; Liao et al., 2018). Those authors suggested that the aggregate size was determining the microbial biomass composition. In particular, Jiang et al. (2011) did not find different patterns of soil microbial biomass, fungal and bacterial biomass in relation to proportion of aggregate size classes and concluded that soil microbial biomass and community structure associated with aggregates was most probably determined by the size of aggregates at this scale (mm). We interpret our data differently in the light of the relationship between differences observed in the relationships between F:B ratio and LM in the different treatments. We would surmise that the negative relationship between F:B and LM in the DD treatment –especially when combined with irrigation– may be due to increased earthworm-induced bioturbation, also corroborated by the little propensity to form LM at increasing F:B ratio (Giannopoulos et al., 2010; Thomas et al., 2020). In fact, this would be corroborated by the significantly higher earthworm density under DD than IT considering all seven earthworm counts conducted over from 2003 and 2015 at the experimental site (Tregurtha and Richards, 2017).

The rainfed IT trend line for F:B *vs.* OC-LM was decreasing while other treatments showed no trend or a positive trend of increasing. Increasing fungal biomass has been postulated to increase SOC sequestration (Sae-Tun et al., 2022). The effects of intensive tillage have generally been shown to have negative effects on the fungal community (e.g., Sharma-Poudyal et al., 2017; Sae-Tun et al., 2022) while irrigation appeared to be more unpredictable (e.g. Lü et al., 2020; Lambie et al., 2021; Bhandari et al., 2022). We surmise that in this case, irrigation had a positive effect on the fungal community and partially ameliorated the deleterious effects of intensive tillage. It must also be noted, however, that different fungal specifies (or traits associated with fungal groups) appear to have varying degrees of soil aggregate formation potential (e.g., Daynes et al., 2012; Lehmann et al., 2020), so that the actual composition of the fungal groups (particularly for AM fungi) is likely to play a role in the degree to which the fungal biomass promotes formation of LM. Several authors (e.g., Chung et al., 2010; Six and Paustian, 2014) found that the SOC stored in microaggregates within macroaggregates and s+c fractions is a general diagnostic of SOC storage capacity under contrasting management systems that have reached

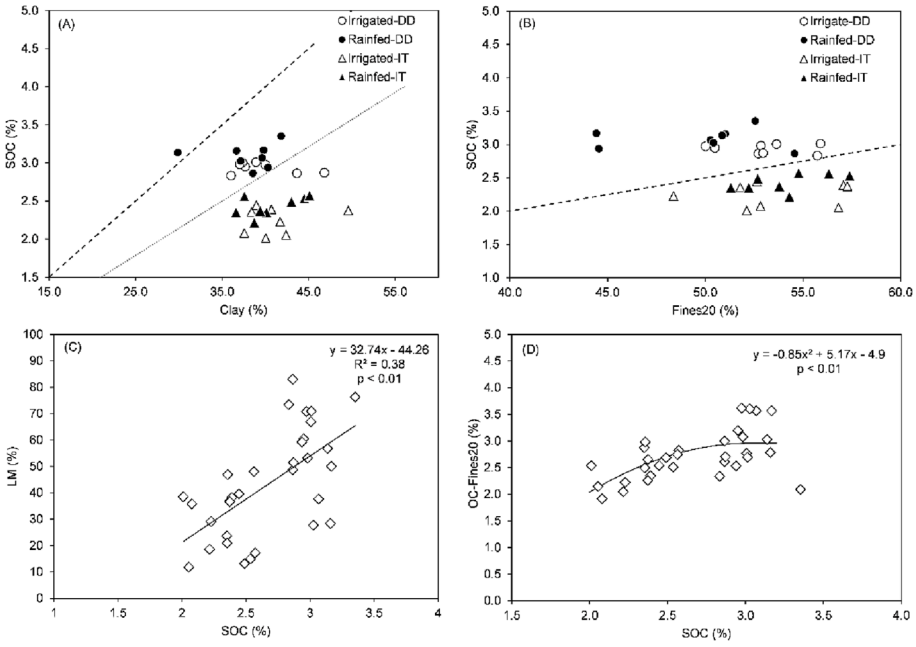

Fig. 4. Relationship between (A) clay, and (B) Fines20 particles and total soil organic carbon (SOC) contents under different management practices: Irrigated and Rainfed, intensive tillage (IT) and direct drill (DD). The dashed lines separate soil samples into samples with clay:SOC and Fines20:SOC ratios below and above the saturation thresholds of 10 and 20 according to Dexter et al. (2008) and Hassink (1997), respectively. The dotted line (A) indicates that a saturation threshold of 14 for the clay:SOC ratio would result in the same separation as the Dexter threshold. The relationship between total SOC and LM (C) as well as SOC and the OC-Fines20 particles (D) is also reported. Data points represent individual sampling points.

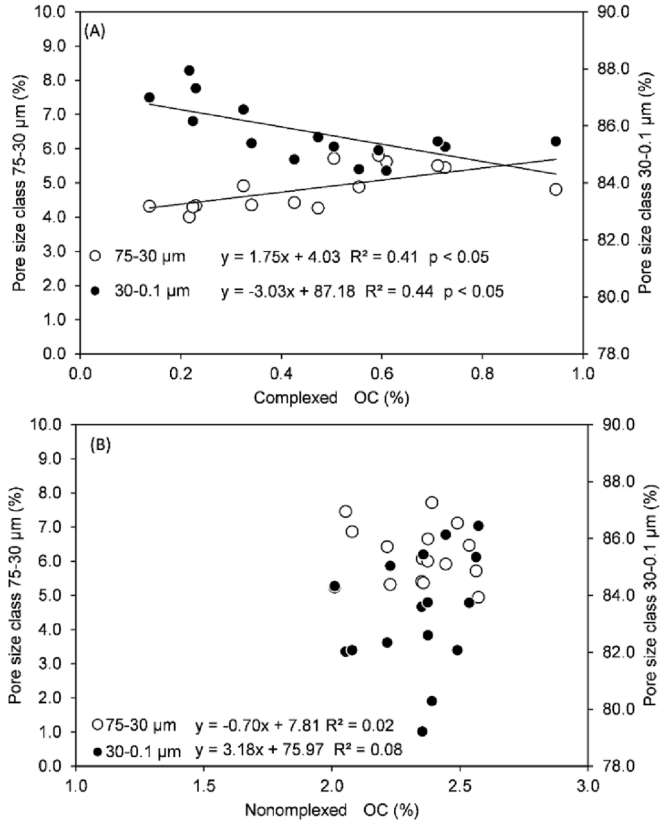

Fig. 5. Relationship between soil pore classes and (A) complexed organic carbon, (B) noncomplexed OC (derived using the Fines20:SOC threshold). Data points represent individual sampling points.

equilibrium, such as in intensive tillage compared with no-tillage. In our experiment, we did not observe SOC differences in any aggregate size class < 250 µm (OC-m and OC-s+c) under the two different tillage practices, suggesting that a SOC-aggregation equilibrium was likely not reached yet, even after more than a decade of continuous soil tillage management (Gulde et al., 2008). On the other hand, complementary functional properties of the structure of aggregate classes such as pore connectivity or tortuosity were not investigated (Young et al., 2001), suggesting that further investigations are required to confirm our results and validate the aggregate hierarchy model. Regarding the role of mineralogical composition, Denef et al. (2004) reported that the link between SM and OC-m stabilization had a lesser effect in soils dominated by 1:1 clay minerals because of both positive and negative charges coexist, and the formation of stable aggregates occurs through mineral–mineral binding regardless of the SOC content. In contrast, in soils dominated by 2:1 clay mineral –like in our soils (Table 3)– organic matter is the primary factor for forming stable bonds with clay, mediated by positively charged cations. Moreover, it can be excluded that the lack of differences between DD and IT was due to differences in the soil mineralogical composition that might result from contrasting tillage, i.e., soil layer inversion with ploughing *vs*. no tillage. In fact, soil mineralogical composition of all treatments was similar.

Beyond aggregate breakdown, some additional differences in soil structural changes were observed between DD and IT, which could be associated with differences in the SOC content therein. The IT generated slightly more rounded SM with more convex closure and a higher convexity compared to DD (Fig. 2, Table 7), meaning that the external aggregate structure was free of irregular features. This might suggest that free organic matter particles capable of forming stable macroaggregates (Six et al., 2002) were lacking due to IT mechanical disturbance which increased friction between aggregates (Alvarez et al., 2012) and between aggregates and machineries, thereby slowing down soil aggregation processes. Moreover, some significant lower pore size class (75–30 µm) in IT than DD might be associated with some slight increase of the smaller pore classes (µm 30–5 and 5–01 µm) under DD than IT. This would suggest a larger SOC mineralization protection mechanisms under DD than under IT (Simonetti et al., 2017), being i) enhanced by fine particle-OC interactions, and, at the same time, ii) enhanced SOC occlusion within aggregates (von Lutzow et al., 2006).

4.2. Long-term irrigation effects on soil aggregation, SOC concentration and microbial community

Similar to tillage, different irrigation treatments modified only LM, corroborating previous findings from the literature. For instance, our observation about higher LM under Irrigated than Rainfed management

was also found by Blanco-Canqui et al. (2010), who reported an increase in the proportion of macroaggregates and the associated decrease of microaggregates under irrigated systems. Similar results were also reported in another experiment after a decade of rainfed *vs.* irrigation management in a semi-arid environment in Argentina (Giubergia et al., 2013). In our study, the SOC content as well as the total PLFA biomass in Irrigated and Rainfed treatments was comparable contradicting previous findings. For instance, Pareja-Sánchez et al. (2020) highlighted that irrigation led to increased biomass production after conversion from rainfed cropping system, with more C inputs from greater productivity of the cropping system devoted to maize production. Even in our experiment Irrigation treatment led to significantly higher annual yields throughout the crop rotation (Müller et al., 2019), but the OC content between aggregate size classes were similar. As observed for the results related to different tillage intensity treatments, it is likely that the dynamics responsible for forming OC-soil particles structures were still unstable after 14 years, and that the expected differentiation between irrigation and rainfed management on SOC that in turn would result in a different aggregate stabilization was masked.

4.3. Relationship between soil particles and SOC concentration

Despite slight variations between treatments at the aggregate scale, the relationship between SOC and soil fine particles suggests that some SOC saturation dynamics occurred (Fig. 4). Especially, the Fines20:SOC ratio = 20 (Hassink, 1997; Schjønning et al., 2018) separated treatments, with all DD soils exceeding the saturation threshold, and conversely, all IT soils not reaching the thresholds, emphasizing that non-complexed OC occurred only under DD. In contrast the clay:SOC ratio = 10 as suggested by Dexter et al. (2008) did not differentiate between treatments. Only when the saturation threshold was set to 14, the separation of samples in the treatments was identical to that of the Fines20:SOC ratio separation. As previously reported by Dexter et al. (2008), who found that most of their samples taken from permanent grassland soils or untilled soils were below the saturation threshold, soils cultivated at low intensity were clearly separated from conventional high intensity systems in our study. The discrepancy between our clay:SOC ratio and that suggested by Dexter et al. (2008) could be related to, e.g., differences in clay content and mineralogy with respect to those at our experimental site. Similar results were already described in previous publications (Fernández-Ugalde et al., 2016; Getahun et al., 2016; Johannes et al., 2017), highlighting the influence of site-specific conditions.

Separating treatments according to complexed and non-complexed OC with soil particles involved a distinction in the soil structure formation that arose from pore size distribution analysis. In fact, an increase of complexed OC was associated with a lower frequency of smaller pores (30–0.01 μm) and a higher frequency of larger pores (75–30 μm), with implications on pore space reallocation with a shift from small to large pores (Schlüter et al, 2011). This dynamic was observed until Fines20 reached saturation in OC content, beyond which the amount of additional non-complexed OC –which only occurred under DD treatment– did not provide any further change in these soil physical properties (Fig. 5). Nevertheless, only further, more in-depth studies under the same soil tillage intensity could confirm that what was observed was indeed the effect of SOC alone and was not related to tillage. In fact, differences between complexed and non-complexed OC were also associated with different tillage conditions that could have created a change in the degree of disturbance, despite some authors emphasized that the effect of tillage is mostly found in pores > 200 μm (Lipiec et al., 2006). In this context, the aggregation structure showed that OC-LM was stored differently between DD and IC, but not between Irrigated and Rainfed, even though their mass contributions differed to a similar magnitude. Still, it remains unclear whether differences in microbial dynamics were affected by tillage-induced or SOC-induced pore structure changes, which could have modified the movement of soil organisms and compromised the microbial accessibility of SOC located in the smaller pores of about 0.2 μm (Six et al., 2006). To note is that when a threshold value of 10 (i.e., the clay:SOC ratio) was used as a predictor of non-complexed OC, no SOC-mediated structure differences were observed, which is in line with previous findings (Schjønning et al., 2012), while Fines20 was a better predictor of soil structural properties than clay. Moreover, OC bound to the physically separated Fines20 was nonlinearly associated with total SOC content, corroborating previous findings (Lugato et al., 2010) where an asymptotic relationship was found when the complexed OC content was close to saturation. It follows that the mineral fraction tended to be close to SOC-saturation, and that additional SOC was likely accumulated in more labile forms (Gulde et al., 2008).

5. Conclusions

In the present study, we discuss effects of tillage and irrigation on soil aggregation and carbon storage both from a biological perspective (i.e., the relationship of fungal biomass to aggregate structure) and also from the purely physicochemical perspective. Our results show that 14 years of continuous no tillage (DD) has not likely determined SOC-structure steady-state conditions compared to conventional practices (IT) in a New Zealand Cambisol, despite a significant difference in topsoil SOC (DD = 30.1 ± 0.3; IT = 23.4 ± 0.4 g kg^{-1}), suggesting that additional SOC accumulation is likely possible. Similarly, Irrigation *vs.* Rainfed managements did not highlight significant effects on soil structure and SOC content. The variability between aggregate size classes < 250 μm between treatments was also insignificant, suggesting the continuation of transitory aggregate formation processes that were not stabilized yet. Thus, our initial hypothesis of detrimental effects on soil structure and SOC accumulation of both tillage and irrigation was not fully demonstrated yet. However, a SOC saturation threshold was likely reached under DD, suggesting that additional non-complexed OC was likely unprotected. In this context, the analysis of soil particles revealed that Fines20 was a better predictor of SOC saturation threshold than clay alone, the former probably reflecting OC-soil interactions better and being most important for determining soil physical quality. Our results also suggest that fungi are important for the initial large aggregate formation in soils after cultivation. Further studies should investigate these dynamics in a longer time frame and at greater depths beyond the surface layer alone, to better understand the potential of SOC storage.

Declaration of Competing Interest

The authors declare that they have no known competing financial interests or personal relationships that could have appeared to influence the work reported in this paper.

Data availability

Data will be made available on request.

Acknowledgments

The authors are grateful to Dr. Carlo Camarotto and Dr. Matteo Longo from DAFNAE for the soil particle characterization. This project was funded through the New Zealand Ministry for Business Innovation and Education (Contract 34573) and the European-RISE project 'PROTINUS' (Contract 645717) with counter-funding from the Royal Society of New Zealand. The authors also thank FAR for access to the experimental study.

Appendix A. Supplementary data

Supplementary data to this article can be found online at https://doi.org/10.1016/j.geoderma.2023.116398.

References

Almagro, M., Garcia-Franco, N., Martínez-Mena, M., 2017. The potential of reducing tillage frequency and incorporating plant residues as a strategy for climate change mitigation in semiarid Mediterranean agroecosystems. Agric. Ecosyst. Environ. 246, 210–220. https://doi.org/10.1016/j.agee.2017.05.016.

Alvarez, M.F., Osterrieth, M.L., Del Rio, J.L., 2012. Changes on aggregates morphology and roughness induced by different uses of Typical Argiudolls, Buenos Aires province. Argentina. Soil Tillage Res. 119, 38–49. https://doi.org/10.1016/j.still.2011.12.003.

Bååth, E., Anderson, T.H., 2003. Comparison of soil fungal/bacterial ratios in a pH gradient using physiological and PLFA-based techniques. Soil Biol. Biochem. 35, 955–963. https://doi.org/10.1016/S0038-0717(03)00154-8.

Balesdent, J., Chenu, C., Balabane, M., 2000. Relationship of soil organic matter dynamics to physical protection and tillage. Soil Tillage Res. 53, 215–230. https://doi.org/10.1016/S0167-1987(99)00107-5.

Bardgett, R.D., Hobbs, P.J., Frostegård, Å., 1996. Changes in soil fungal:bacterial biomass ratios following reductions in the intensity of management of an upland grassland. Biol. Fertil. Soils 1996 223 22, 261–264. https://doi.org/10.1007/BF00382522.

Bhandari, K.B., Acosta-Martínez, V., Pérez-Guzmán, L., West, C.P., 2022. Soil health within transitions from irrigation to limited irrigation and dryland management. Agric. Environ. Lett. 7 (1), e20077.

Bittelli, M., Andrenelli, M.C., Simonetti, G., Pellegrini, S., Artioli, G., Piccoli, I., Morari, F., 2019. Shall we abandon sedimentation methods for particle size analysis in soils? Soil Tillage Res. 185, 36–46. https://doi.org/10.1016/J.STILL.2018.08.018.

Blanco-Canqui, H., Klocke, N.L., Schlegel, A.J., Stone, L.R., Rice, C.W., 2010. Impacts of Deficit Irrigation on Carbon Sequestration and Soil Physical Properties under No-Till. Soil Sci. Soc. Am. J. 74, 1301–1309. https://doi.org/10.2136/sssaj2009.0364.

Bligh, E.G., Dyer, W.J., 1959. A rapid method of total lipid extraction and purification. Can. J. Biochem. Physiol. 37, 911–917.

Cambardella, C.A., Elliott, E.T., 1992. Particulate Soil Organic-Matter Changes across a Grassland Cultivation Sequence. Soil Sci. Soc. Am. J. 56, 777–783. https://doi.org/10.2136/sssaj1992.03615995005600030017x.

Cameron, K.C., Buchan, G.D., 2006. Porosity and pore size distribution. Encycl. soil Sci. Fr. London 1350–1353.

Chenu, C., Angers, D.A., Barré, P., Derrien, D., Arrouays, D., Balesdent, J., 2018. Increasing organic stocks in agricultural soils: Knowledge gaps and potential innovations. Soil Tillage Res. 188, 41–52. https://doi.org/10.1016/J.STILL.2018.04.011.

Chung, H., Grove, J.H., Six, J., 2008. Indications for Soil Carbon Saturation in a Temperate Agroecosystem. Soil Sci. Soc. Am. J. 72, 1132–1139. https://doi.org/10.2136/sssaj2007.0265.

Chung, H., Ngo, K.J., Plante, A., Six, J., 2010. Evidence for carbon saturation in a highly structured and organic-matter-rich soil. Soil Science Society of America Journal 74 (1), 130–138.

Dal Ferro, N., Berti, A., Francioso, O., Ferrari, E., Matthews, G.P., Morari, F., 2012. Investigating the effects of wettability and pore size distribution on aggregate stability: The role of soil organic matter and the humic fraction. Eur. J. Soil Sci. 63 https://doi.org/10.1111/j.1365-2389.2012.01427.x.

Daynes, C.N., Zhang, N., Saleeba, J.A., McGee, P.A., 2012. Soil aggregates formed in vitro by saprotrophic Trichocomaceae have transient water-stability. Soil Biol. Biochem. 48, 151–161. https://doi.org/10.1016/J.SOILBIO.2012.01.010.

Daynes, C.N., Field, D.J., Saleeba, J.A., Cole, M.A., McGee, P.A., 2013. Development and stabilisation of soil structure via interactions between organic matter, arbuscular mycorrhizal fungi and plant roots. Soil Biol. Biochem. 57, 683–694.

Denef, K., Six, J., Merckx, R., Paustian, K., 2004. Carbon Sequestration in Microaggregates of No-Tillage Soils with Different Clay Mineralogy. Soil Sci. Soc. Am. J. 68, 1935–1944. https://doi.org/10.2136/sssaj2004.1935.

Dexter, A.R., Richard, G., Arrouays, D., Czyż, E.A., Jolivet, C., Duval, O., 2008. Complexed organic matter controls soil physical properties. Geoderma 144, 620–627. https://doi.org/10.1016/J.GEODERMA.2008.01.022.

Drewry, J.J., Carrick, S., Penny, V., Dando, J.L., Koele, N., 2022. Effect of irrigation on soil physical properties on temperate pastoral farms: a regional New Zealand study. Soil Res. 60 (8), 760–771. https://doi.org/10.1071/SR21254.

Elliott, E.T., 1986. Aggregate Structure and Carbon, Nitrogen, and Phosphorus in Native and Cultivated Soils. Soil Sci. Soc. Am. J. 50, 627–633. https://doi.org/10.2136/sssaj1986.03615995005000030017x.

Fernández-Ugalde, O., Barré, P., Virto, I., Hubert, F., Billiou, D., Chenu, C., 2016. Does phyllosilicate mineralogy explain organic matter stabilization in different particle-size fractions in a 19-year C3/C4 chronosequence in a temperate Cambisol? Geoderma 264, 171–178. https://doi.org/10.1016/j.geoderma.2015.10.017.

Garcia-Franco, N., Martínez-Mena, M., Goberna, M., Albaladejo, J., 2015. Changes in soil aggregation and microbial community structure control carbon sequestration after afforestation of semiarid shrublands. Soil biol. biochem. 87, 110–121.

Garcia-Franco, N., Hobley, E., Hübner, R., Wiesmeier, M., 2018. Climate-smart soil management in semiarid regions. In: Soil management and climate change. Academic Press, pp. 349–368.

Garcia-Franco, N., Wiesmeier, M., Hurtarte, L.C.C., Fella, F., Martínez-Mena, M., Almagro, M., Kögel-Knabner, I., 2021. Pruning residues incorporation and reduced tillage improve soil organic matter stabilization and structure of salt-affected soils in a semi-arid Citrus tree orchard. Soil Till. Res. 213, 105129.

Getahun, G.T., Munkholm, L.J., Schjønning, P., 2016. The influence of clay-to-carbon ratio on soil physical properties in a humid sandy loam soil with contrasting tillage and residue management. Geoderma 264, 94–102. https://doi.org/10.1016/j.geoderma.2015.10.002.

Ghani, A., Dexter, M., Perrott, K.W., 2003. Hot-water extractable carbon in soils: a sensitive measurement for determining impacts of fertilisation, grazing and cultivation. Soil Biol. Biochem. 35, 1231–1243. https://doi.org/10.1016/S0038-0717(03)00186-X.

Giannopoulos, G., Pulleman, M.M., Van Groenigen, J.W., 2010. Interactions between residue placement and earthworm ecological strategy affect aggregate turnover and N_2O dynamics in agricultural soil. Soil Biol. Biochem. 42, 618–625.

Giubergia, J.P., Martellotto, E., Lavado, R.S., 2013. Complementary irrigation and direct drilling have little effect on soil organic carbon content in semiarid Argentina. Soil Tillage Res. 134, 147–152. https://doi.org/10.1016/j.still.2013.08.003.

Goh, K.M., 2004. Carbon sequestration and stabilization in soils: Implications for soil productivity and climate change. Soil Science and Plant Nutrition 50 (4), 467–476.

Gulde, S., Chung, H., Amelung, W., Chang, C., Six, J., 2008. Soil Carbon Saturation Controls Labile and Stable Carbon Pool Dynamics. Soil Sci. Soc. Am. J. 72, 605–612. https://doi.org/10.2136/sssaj2007.0251.

Guo, L., Shen, J., Li, B., Li, Q., Wang, C., Guan, Y., Tang, X., 2020. Impacts of agricultural land use change on soil aggregate stability and physical protection of organic C. Sci. Tot. Environ. 707, 136049.

Hassink, J., 1997. The capacity of soils to preserve organic C and N by their association with clay and silt particles. Plant Soil 191, 77–87. https://doi.org/10.1023/A:1004213929699.

Helgason, B.L., Gregorich, E.G., Janzen, H.H., Ellert, B.H., Lorenz, N., Dick, R.P., 2014. Long-term microbial retention of residue C is site-specific and depends on residue placement. Soil Biol Biochem. 68, 231–240.

Hewitt, A.E., 2010. New Zealand Soil Classification, Landcare R. ed. Manaaki Whenua Press.

Hondebrink, M.A., Cammeraat, L.H., Cerdà, A., 2017. The impact of agricultural management on selected soil properties in citrus orchards in Eastern Spain: A comparison between conventional and organic citrus orchards with drip and flood irrigation. Sci. Tot. Environ. 581, 153–160.

IUSS Working Group WRB, World Reference Base for Soil Resources 2014, update 2015. International soil classification system for naming soils and creating legends for soil maps. World Soil Resources Reports No. 106. FAO, Rome.

Jastrow, J.D., Miller, R.M., Lussenhop, J., 1998. Contributions of interacting biological mechanisms to soil aggregate stabilization in restored prairie. Soil Biol. Biochem. 30, 905–916. https://doi.org/10.1016/S0038-0717(97)00207-1.

Jiang, X., Wright, A.L., Wang, X., Liang, F., 2011. Tillage-induced changes in fungal and bacterial biomass associated with soil aggregates: A long-term field study in a subtropical rice soil in China. Appl. Soil Ecol. 48, 168–173. https://doi.org/10.1016/J.APSOIL.2011.03.009.

Johannes, A., Matter, A., Schulin, R., Weisskopf, P., Baveye, P.C., Boivin, P., 2017. Optimal organic carbon values for soil structure quality of arable soils. Does clay content matter? Geoderma 302, 14–21. https://doi.org/10.1016/j.geoderma.2017.04.021.

Kassam, A., Friedrich, T., Derpsch, R., 2019. Global spread of conservation agriculture. Int. J. Environ. Stud. 76 (1), 29–51. https://doi.org/10.1080/00207233.2018.1494927.

Kemper, W.D., Rosenau, R.C., 1986. Aggregate stability and size distribution. In: Klute, A. (Ed.), Methods of Soil Analysis: Part 1 Physical and Mineralogical Methods. ASA and SSSA, Madison, WI, pp. 425–442.

Kochsiek, A.E., Knops, J.M., Walters, D.T., Arkebauer, T.J., 2009. Impacts of management on decomposition and the litter-carbon balance in irrigated and rainfed no-till agricultural systems. Agric. Forest Meteorol. 149 (11), 1983–1993. https://doi.org/10.1016/j.agrformet.2009.07.004.

Kool, D.M., Chung, H., Tate, K.R., Ross, D.J., Newton, P.C., Six, J., 2007. Hierarchical saturation of soil carbon pools near a natural CO_2 spring. Global Change Biol. 13 (6), 1282–1293.

Kunze, G.W., Dixon, J.B., 1986. Pretreatment for Mineralogical Analysis. In: Kluite, A. (Ed.), Methods of Soil Analysis: Part 1 Physical and Mineralogical Methods. John Wiley & Sons Ltd, Madison, USA, pp. 91–100. https://doi.org/10.2136/sssabookser5.1.2ed.c5.

Lambie, S.M., Mudge, P.L., Stevenson, B.A., 2021. Microbial community composition and activity in paired irrigated and non-irrigated pastures in New Zealand. Soil Res. 60 (4), 337–348.

Lehmann, A., Zheng, W., Rillig, M.C., 2017. Soil biota contributions to soil aggregation. Nat. Ecol. Evol. 2017 112 1, 1828–1835. Doi: 10.1038/s41559-017-0344-y.

Lehmann, A., Zheng, W., Ryo, M., Soutschek, K., Roy, J., Rongstock, R., Maaß, S., Rillig, M.C., 2020. Fungal Traits Important for Soil Aggregation. Front. Microbiol. 10, 2904. https://doi.org/10.3389/FMICB.2019.02904/BIBTEX.

Liao, H., Zhang, Y., Zuo, Q., Du, B., Chen, W., Wei, D., Huang, Q., 2018. Contrasting responses of bacterial and fungal communities to aggregate-size fractions and long-term fertilizations in soils of northeastern China. Sci. Total Environ. 635, 784–792. https://doi.org/10.1016/J.SCITOTENV.2018.04.168.

Liao, H., Zhang, Y., Wang, K., Hao, X., Chen, W., Huang, Q., 2020. Complexity of bacterial and fungal network increases with soil aggregate size in an agricultural Inceptisol. Appl. Soil Ecol. 154, 103640 https://doi.org/10.1016/J.APSOIL.2020.103640.

Lipiec, J., Kuś, J., Słowińska-Jurkiewicz, A., Nosalewicz, A., 2006. Soil porosity and water infiltration as influenced by tillage methods. Soil Till. Res. 89 (2), 210–220. https://doi.org/10.1016/j.still.2005.07.012.

Liu, A., Ma, B.L., Bomke, A.A., 2005. Effects of Cover Crops on Soil Aggregate Stability, Total Organic Carbon, and Polysaccharides. Soil Sci. Soc. Am. J. 69, 2041–2048. https://doi.org/10.2136/sssaj2005.0032.

Lü, P.P., Zheng, Y., Chen, L., Ji, N.N., Yao, H., Maitra, P., Guo, L.D., 2020. Irrigation and fertilization effects on arbuscular mycorrhizal fungi depend on growing season in a dryland maize agroecosystem. Pedobiologia 83, 150687.

Lugato, E., Simonetti, G., Morari, F., Nardi, S., Berti, A., Giardini, L., 2010. Distribution of organic and humic carbon in wet-sieved aggregates of different soils under long-term fertilization experiment. Geoderma 157, 80–85. https://doi.org/10.1016/j.geoderma.2010.03.017 ER.

Mudge, P.L., Kelliher, F.M., Knight, T.L., O'Connell, D., Fraser, S., Schipper, L.A., 2017. Irrigating grazed pasture decreases soil carbon and nitrogen stocks. Glob. Chang. Biol. 23, 945–954. https://doi.org/10.1111/GCB.13448.

Müller, K., Dal Ferro, N., Katuwal, S., Tregurtha, C., Zanini, F., Carmignato, S., Wollesen de Jonge, L., Moldrup, P., Morari, F., 2019. Effect of long-term irrigation and tillage practices on X-ray CT and gas transport derived pore-network characteristics. Soil Res. 57, 657. https://doi.org/10.1071/SR18210.

Olsson, P.A., 1999. Signature fatty acids provide tools for determination of the distribution and interactions of mycorrhizal fungi in soil. FEMS Microbiol. Ecol. 29, 303–310. https://doi.org/10.1111/J.1574-6941.1999.TB00621.X.

Olsson, P.A., Bååth, E., Jakobsen, I., Söderström, B., 1995. The use of phospholipid and neutral lipid fatty acids to estimate biomass of arbuscular mycorrhizal fungi in soil. Mycol. Res. 99, 623–629. https://doi.org/10.1016/S0953-7562(09)80723-5.

Pareja-Sánchez, E., Plaza-Bonilla, D., Ramos, M.C., Lampurlanés, J., Álvaro-Fuentes, J., Cantero-Martínez, C., 2017. Long-term no-till as a means to maintain soil surface structure in an agroecosystem transformed into irrigation. Soil Tillage Res. 174, 221–230. https://doi.org/10.1016/j.still.2017.07.012.

Pareja-Sánchez, E., Cantero-Martínez, C., Álvaro-Fuentes, J., Plaza-Bonilla, D., 2020. Soil organic carbon sequestration when converting a rainfed cropping system to irrigated corn under different tillage systems and N fertilizer rates. Soil Sci. Soc. Am. J. 84 (4), 1219–1232. https://doi.org/10.1002/saj2.20116.

Piccoli, I., Chiarini, F., Carletti, P., Furlan, L., Lazzaro, B., Nardi, S., Berti, A., Sartori, L., Dalconi, M.C., Morari, F., 2016. Disentangling the effects of conservation agriculture practices on the vertical distribution of soil organic carbon. Evidence of poor carbon sequestration in North- Eastern Italy. Agric. Ecosyst. Environ. 230, 68–78. https://doi.org/10.1016/j.agee.2016.05.035.

Rillig, M.C., Mummey, D.L., 2006. Mycorrhizas and soil structure. New Phytol. 171, 41–53. https://doi.org/10.1111/J.1469-8137.2006.01750.X.

Ritz, K., Young, I.M., 2004. Interactions between soil structure and fungi. Mycologist 18, 52–59. https://doi.org/10.1017/S0269915X04002010.

Rosa, L., 2022. Adapting agriculture to climate change via sustainable irrigation: Biophysical potentials and feedbacks. Environ. Res. Lett. 17 (6), 063008 https://doi.org/10.1088/1748-9326/ac7408.

Sae-Tun, O., Bodner, G., Rosinger, C., Zechmeister-Boltenstern, S., Mentler, A., Keiblinger, K., 2022. Fungal biomass and microbial necromass facilitate soil carbon sequestration and aggregate stability under different soil tillage intensities. App. Soil Ecol. 179, 104599 https://doi.org/10.1016/j.apsoil.2022.104599.

Schjønning, P., de Jonge, L.W., Munkholm, L.J., Moldrup, P., Christensen, B.T., Olesen, J. E., 2012. Clay Dispersibility and Soil Friability-Testing the Soil Clay-to-Carbon Saturation Concept. Vadose Zo. J. 11 https://doi.org/10.2136/vzj2011.0067.

Schjønning, P., Jensen, J.L., Bruun, S., Jensen, L.S., Christensen, B.T., Munkholm, L.J., Knudsen, L., 2018. The role of soil organic matter for maintaining crop yields: Evidence for a renewed conceptual basis. Adv. Agron. 150, 35–79.

Schlüter, S., Weller, U., Vogel, H.J., 2011. Soil-structure development including seasonal dynamics in a long-term fertilization experiment. J. Plant Nutr. Soil Sci. 174 (3), 395–403. https://doi.org/10.1002/jpln.201000103.

Sharma-Poudyal, D., Schlatter, D., Yin, C., Hulbert, S., Paulitz, T., 2017. Long-term no-till: a major driver of fungal communities in dryland wheat cropping systems. PLoS one 12 (9), e0184611.

Simonetti, G., Francioso, O., Dal Ferro, N., Nardi, S., Berti, A., Morari, F., 2017. Soil porosity in physically separated fractions and its role in SOC protection. J. Soils Sediments 17, 70–84. https://doi.org/10.1007/s11368-016-1508-0.

Sithole, N.J., Magwaza, L.S., Thibaud, G.R., 2019. Long-term impact of no-till conservation agriculture and N-fertilizer on soil aggregate stability, infiltration and distribution of C in different size fractions. Soil Tillage Res. 190, 147–156. https://doi.org/10.1016/j.still.2019.03.004.

Six, J., Elliott, E.T., Paustian, K., 2000. Soil macroaggregate turnover and microaggregate formation: A mechanism for C sequestration under no-tillage agriculture. Soil Biol. Biochem. 32, 2099–2103. https://doi.org/10.1016/S0038-0717(00)00179-6.

Six, J., Conant, R.T., Paul, E.A., Paustian, K., 2002. Stabilization mechanisms of soil organic matter: Implications for C-saturation of soils. Plant Soil 241, 155–176.

Six, J., Frey, S.D., Thiet, R.K., Batten, K.M., 2006. Bacterial and fungal contributions to carbon sequestration in agroecosystems. Soil Sci. Soc. Am. J. 70 (2), 555–569.

Six, J., Paustian, K., 2014. Aggregate-associated soil organic matter as an ecosystem property and a measurement tool. Soil Biol. Biochem. 68 https://doi.org/10.1016/j.soilbio.2013.06.014.

Stewart, C.E., Paustian, K., Conant, R.T., Plante, A.F., Six, J., 2007. Soil carbon saturation: concept, evidence and evaluation. Biogeochemistry 86, 19–31. https://doi.org/10.1007/s10533-007-9140-0.

Stewart, C.E., Paustian, K., Conant, R.T., Plante, A.F., Six, J., 2008. Soil carbon saturation: evaluation and corroboration by long-term incubations. Soil Biol. Biochem. 40 (7), 1741–1750.

Thomas, E., Shanthi, P.V., Kurien, V.T., Thomas, A.P., 2020. The potential of earthworms in soil carbon storage: a review. Environ. Exp. Biol. 18, 61–75.

Tregurtha, C., Richards, K.K., 2017. Soil quality monitoring of the FAR Chertsey Cultivation Trial – analysis of results from 2004–2017. A Plant & Food Research report prepared for Foundation for Arable Research.

B. Trost A. Prochnow K. Drastig A. Meyer-Aurich F. Ellmer M. Baumecker Irrigation, soil organic carbon and N2O emissions 2013 Agron. Sustain. Dev A review 10.1007/s13593-013-0134-0.

von Lutzow, M., Kogel-Knabner, I., Ekschmitt, K., Matzner, E., Guggenberger, G., Marschner, B., Flessa, H., 2006. Stabilization of organic matter in temperate soils: mechanisms and their relevance under different soil conditions - a review. Eur. J. Soil Sci. 57, 426–445. https://doi.org/10.1111/j.1365-2389.2006.00809.x ER.

Waldrop, M.P., Firestone, M.K., 2004. Microbial community utilization of recalcitrant and simple carbon compounds: Impact of oak-woodland plant communities. Oecologia 138, 275–284. https://doi.org/10.1007/S00442-003-1419-9/FIGURES/7.

White, D.C., Davis, W.M., Nickels, J.S., King, J.D., Bobbie, R.J., 1979. Determination of the sedimentary microbial biomass by extractible lipid phosphate. Oecologia 1979 401 40, 51–62. Doi: 10.1007/BF00388810.

Whitehead, D., Schipper, L.A., Pronger, J., Moinet, G.Y.K., Mudge, P.L., Calvelo Pereira, R., Kirschbaum, M.U.F., McNally, S.R., Beare, M.H., Camps-Arbestain, M., 2018. Management practices to reduce losses or increase soil carbon stocks in temperate grazed grasslands: New Zealand as a case study. Agric. Ecosyst. Environ. 265, 432–443. https://doi.org/10.1016/J.AGEE.2018.06.022.

Wiesmeier, M., Hübner, R., Spörlein, P., Geuß, U., Hangen, E., Reischl, A., Kögel-Knabner, I., 2014. Carbon sequestration potential of soils in southeast Germany derived from stable soil organic carbon saturation. Global change biology 20 (2), 653–665.

Wiesmeier, M., Urbanski, L., Hobley, E., Lang, B., von Lützow, M., Marin-Spiotta, E., van Wesemael, B., Rabot, E., Ließ, M., Garcia-Franco, N., Wollschläger, U., Vogel, H.J., Kögel-Knabner, I., 2019. Soil organic carbon storage as a key function of soils - A review of drivers and indicators at various scales. Geoderma. https://doi.org/10.1016/j.geoderma.2018.07.026.

Young, I.M., Crawford, J.W., Rappoldt, C., 2001. New methods and models for characterising structural heterogeneity of soil. Soil Till. Res. 61 (1–2), 33–45. https://doi.org/10.1016/S0167-1987(01)00188-X.

Zelles, L., 1999. Fatty acid patterns of phospholipids and lipopolysaccharides in the characterisation of microbial communities in soil: a review. Biol. Fertil. Soils 1999 292 29, 111–129. https://doi.org/10.1007/S003740050533.

Zhao, L., Sun, Y., Zhang, X., Yang, X., Drury, C.F., 2006. Soil organic carbon in clay and silt sized particles in Chinese mollisols: Relationship to the predicted capacity. Geoderma 132 (3–4), 315–323. https://doi.org/10.1016/j.geoderma.2005.04.026.

Zhou, X., Zhou, L., Nie, Y., Fu, Y., Du, Z., Shao, J., Wang, X., 2016. Similar responses of soil carbon storage to drought and irrigation in terrestrial ecosystems but with contrasting mechanisms: A meta-analysis. Agric. Ecosys. Environ. 228, 70–81.